



e-ISSN: 2278-8875
p-ISSN: 2320-3765

International Journal of Advanced Research

in Electrical, Electronics and Instrumentation Engineering

Volume 10, Issue 7, July 2021

ISSN INTERNATIONAL
STANDARD
SERIAL
NUMBER
INDIA

Impact Factor: 7.282

9940 572 462

6381 907 438

ijareeie@gmail.com

www.ijareeie.com



Improvement of Bandwidth and Gain of a Rectangular Patch Antenna for UWB Applications

M. Firoz Ahmed¹, Abu Zafar Md. Touhidul Islam², M. Hasnat Kabir³

Assistant Professor, Department of Information and Communication Engineering, University of Rajshahi, Bangladesh¹

Professor, Department of Electrical and Electronic Engineering, University of Rajshahi, Bangladesh²

Professor, Department of Information and Communication Engineering, University of Rajshahi, Bangladesh³

ABSTRACT: The crucial drawbacks of a microstrip patch antenna are its limited bandwidth and low gain. A rectangular patch microstrip antenna for UWB applications is proposed in this article, which has been designed to overcome these limitations by embedding right-angle triangular-rectangular slots into the patch and adding a single rectangular slot into the partial ground plane. The antenna is designed on FR-4 substrate with a total size of $30 \times 20 \times 0.8 \text{ mm}^3$, a dielectric constant of 4.4, a thickness of 0.8mm, and a loss tangent of 0.02. The simulation results show that the rectangular patch microstrip antenna (RPMA) with slots achieves a wide bandwidth of 19.7 GHz (3.15 - 22.85 GHz) and a maximum gain of 8.06 dB, which is 16.02 GHz and 3dB greater than the rectangular patch microstrip antenna (RPMA) without slots.

KEYWORDS: Rectangular slot, Right-angle triangular slots, UWB, FR-4 substrate.

I. INTRODUCTION

A microstrip patch antenna (MPA) has significant disadvantages such as narrow bandwidth and low gain, even though it is smaller in size and easy to manufacture [1]. Several studies have been performed in which researchers have demonstrated various strategies and methodologies in order to address the impediments that have also been discussed in the literature review. The greater bandwidth of an antenna is a major challenge in the development of communication, which may radiate across a wide range of frequencies. On the contrary, with a higher gain, an antenna can show better performance. As a result, it is critical to apply specific strategies to overcome the basic problems of the patch antenna. An MPA consists of a substrate with a relative permittivity of ϵ_r and a ground plane. A patch of any shape (rectangular, round, square, elliptical, dipole, and triangular) and size is designed on the substrate [2]. The antennas, manufactured on PCB using microstrip techniques, often work at microwave frequencies. The most frequently used MPAs are rectangular and circular because they give different frequency operations, circular or linear polarization, the versatility of the feedline, and adaptability to array configuration [3]. A feeding line is needed to excite the antenna. Researchers are using different feeding line techniques, like a coaxial probe, microstrip line, aperture coupling, and proximity coupling [4].

We have used microstrip line feeding for our study, in which the microstrip patch is directly aligned with the conducting microstrip feed line (Fig.1). The two most common ways to improve the bandwidth of a microstrip patch antenna are to increase the substrate height or lower the substrate dielectric constant [5]. However, raising the substrate height makes the antenna no longer small, and decreasing the dielectric constant further reduces the resonance, which may cause problems at higher frequencies. In order to improve the gain, a low-loss substrate should be used [6].

In this paper, the antenna is designed in two stages; the first stage is a rectangular patch microstrip antenna (RPMA) without slots, and the second stage is a RPMA with slots. The goals are to improve the gain and bandwidth performance of the antenna.

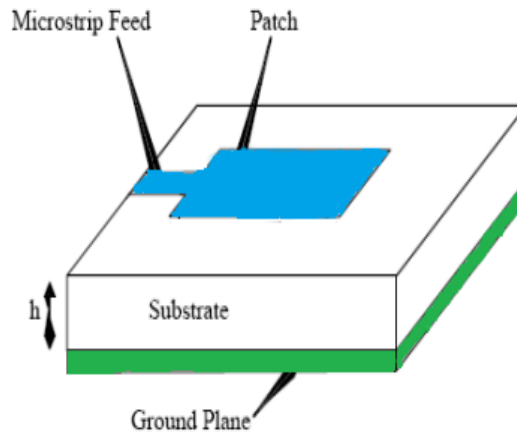


FIGURE 1. Microstrip patch antenna with Microstrip line feeding.

II. LITERATURE REVIEW

A miniaturized size ultra-wideband microstrip antenna based on a metamaterial array was designed for UWB applications by A.F. Darweesh and G.O. Yetkin [7] using computer simulation technology (CST) software. The antenna is $36 \times 38 \times 1.58 \text{ mm}^3$ in size and has a partial ground printed on the FR4 dielectric substrate. The metamaterial array is made up of two triple split-ring resonators that are placed above the antenna structure. The results noted that an improved bandwidth of 2.6 GHz – 20 GHz with a gain of 5.6 dB was achieved. J. Vijayalakshmi and G. Murugesan [8] presented a miniaturized high-gain (MHG) ultra-wideband (UWB) unidirectional monopole antenna with defected ground structure (DGS) for ultra-wideband applications. The MHG antenna is printed on FR4 substrate material and has a total size of $26.6 \text{ mm} \times 29.3 \text{ mm} \times 1.6 \text{ mm}$. It works in the UWB frequency band and has a bandwidth of 3.1 GHz to 10.6 GHz. This antenna shows a peak gain of 7.20 dB with an efficiency of 95% and a bandwidth of 3.2 – 10.6 GHz.

S. Patel and C. Argyropoulos [9] improved bandwidth and gain in a compact microstrip antenna by using multiple corrugated split-ring resonators (SRR) metamaterials. Square teeth have been added to the outer edges of SRR rings in the corrugated designs. The effectiveness of a microstrip antenna loaded with eight different SRR loads is analyzed. Through their investigation, they were capable of achieving a higher bandwidth of 420 MHz with a gain of 7 dB. M. Samsuzzaman, M.T. Islam, and J.S. Mandeep investigated the microstrip patch antenna with a single feed, new shape, compact size, and high gain [10]. The antenna has an overall dimension of $9.5 \text{ mm} \times 7.96 \text{ mm} \times 1.905 \text{ mm}$ and is printed on Rogers RT/duroid 6010 substrate material. The triple equalitarian triangular slot is used to decrease the size of the antenna and enhancing the bandwidth. The antenna achieves a gain of 6 dB and operating bandwidth of 15.27 – 15.72 GHz.

Abbas et al. [11] developed a double-sided printed antenna with a parasitic patch for ultra-wideband (UWB) applications. The antenna is printed on FR4 epoxy substrate material and has an overall size of $30 \times 24.8 \times 1.6 \text{ mm}^3$. It has an asymmetric feed line with an impedance of 50Ω . The antenna shows a 7 dB gain and an 11.51 GHz extended bandwidth ranging from 1.69 to 13.2 GHz. S. Baudha and M.V. Yadav [12] proposed a compact UWB planar antenna with a corrugated ladder ground plane for a variety of applications. The antenna is $15 \times 20 \times 1.5 \text{ mm}^3$ in size and is made on a low-cost, relatively cheap FR-4 substrate with relative permittivity of 4.3, a permeability of 1, and a loss tangent of 0.025. The impedance bandwidth and peak gain of the antenna are 130.4% (2.4 – 11.4 GHz) and 3.5 dB, respectively.

S. Baudha and M.V. Yadav investigated a novel design for UWB applications of a planar antenna with a modified patch and a defective ground plane [13]. The antenna has an optimal dimension of $20 \times 25 \times 1.5 \text{ mm}^3$ and is printed on a FR4 substrate material. The operating bandwidth and maximum gain of the antenna are 110% (3.1 – 10.8 GHz) and 5.1 dB, respectively. Tan et al. [14] designed a modified UWB antenna with a gain enhancement for wireless applications on a FR4 substrate. The patch of the antenna is embedded with slots to increase radiation characteristics and ensure a wide impedance bandwidth. To provide proper impedance matching over a wide frequency range, two rectangular ring slots are inserted in the ground plane. The antenna has a total size of $55 \text{ mm} \times 56 \text{ mm} \times 1.6 \text{ mm}$ and is



fabricated on a low-cost FR4 substrate. The analysis shows that an impedance bandwidth ranging from 2.2 GHz to more than 12 GHz, which is equal to 138% fractional bandwidth, is achieved with a maximum gain of more than 6.5 dB.

Elajoumi et al.[15] demonstrated that a compact microstrip rectangular antenna with a defected ground structure (DGS) with different positions of the additional patch in the ground can be used to improve bandwidth for UWB applications. The total size of the antenna is 26 mm × 30 mm × 1.6 mm and is designed on a low-cost FR4 substrate. An improved bandwidth of 3 to 15 GHz (133.33%) with a gain of 1.5 – 4.8 dB is shown. Gain enhancement for the exposure system of a rectangular microstrip patch antenna designed with a microstrip array was described by R.D. Mishra and P.K. Singha [16] in order to achieve a gain of 2.8647 – 5.6692 dB. According to Xiong et al.[17], an enhanced ultra-wideband (UWB) and a high gain rectangular antenna were explicitly designed using planar-patterned metamaterial principles. Isolated triangle gaps and crossed gaps are inserted into the antenna's metal patch and ground plane. The size of the antenna is 27.6 × 31.8 mm² and is printed on an F4BM-2 substrate with a thickness of 0.8 mm and a permittivity of 2.2. The antenna achieves broad bandwidth ranging from 3.85 – 15.62 GHz and an average gain of 5.42 dB, with a peak gain of 8.36 dB.

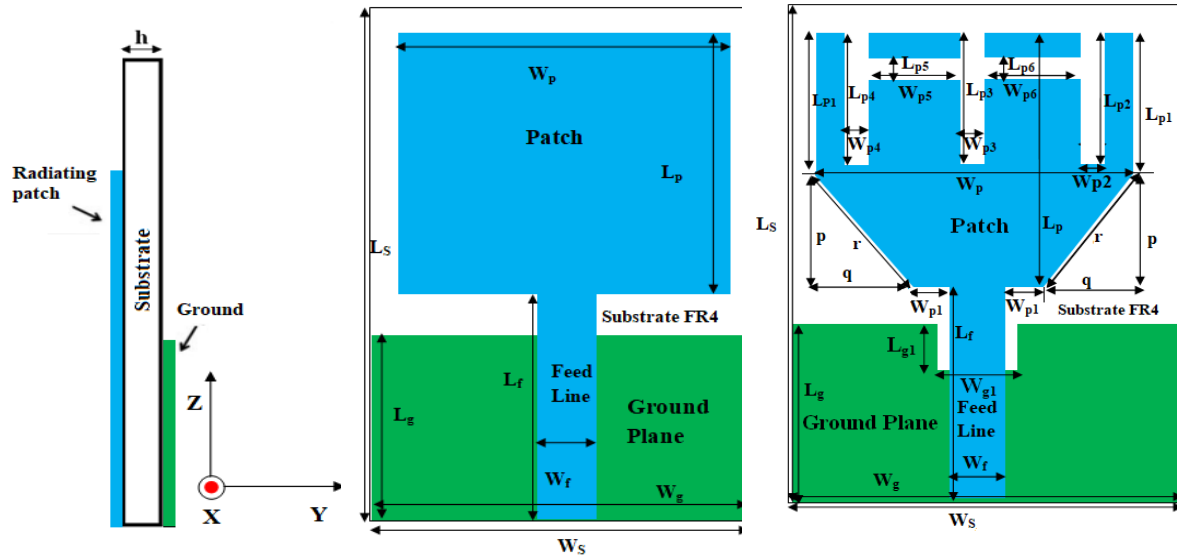
Roy et al. [18] designed a rectangular patch with a width (W) of 32 mm and a length (L) of 24 mm by combining three different geometry shapes, U, E, and H. Alumina 96% is used as the substrate material of the antenna, with a dielectric constant of 9.4 and a loss tangent of 4.0e-4, and it was simulated using Sonnet software. The increase in bandwidth was 4.81% (100 MHz) to 28.71% (610 MHz) for U-shaped patch antenna, 28.89% (630 MHz) for E-shaped patch antenna, and 9.13% (110 MHz) for H-shaped patch antenna. Y. Sung [19] describes how to use a parasitic center patch to increase the bandwidth of a microstrip line-fed printed wide-slot antenna. The antenna, which consists of a rotating square slot and a parasitic patch, is designed on FR4 dielectric substrate with a permittivity of 4.4 and a thickness of 1.6 mm that is commercially available. As a result, an impedance bandwidth of 3.12 GHz (2.23 to 5.35 GHz) and a maximum gain of 4 dB were obtained.

The authors of [20] described a CPW-fed slot antenna on FR4 substrate that can resonate at 5GHz with a gain ranging from -0.98 dB to 4.62 dB. Zhao et al. [21] illustrated a wideband and high gain circularly polarized ultra-high-frequency (UHF) RFID reader microstrip antenna and array with a gain of 9.7 dBi. Lin et al. [22] presented a new design for radio-frequency identification (RFID) tag antenna mounted on a metallic plane with a peak gain of 8.7dBi. In the design of a low-profile two-arm spiral antenna, a circularly symmetric high-impedance surface (HIS) was used as a ground plane [23]. A 11.3% fractional bandwidth is achieved, as well as a maximum gain of 2.5 dB. Rusdiyanto et al. [24] proposed a microstrip antenna design for bandwidth and enhancement purposes that is based on the defected ground structure (DGS) and horizontal patch gap (HPG). The antenna achieved a bandwidth of 764.4 MHz and a gain of 2.8 dBi.

Raviteja et al. [25] investigated the use of U and Quad L-shaped slots with L-shaped DGS and U-shaped dual parasitic elements. This antenna has a bandwidth of 1.40 GHz and a gain of 7.2 dB. A. Swetha and K. R. Naidu [26] introduce a novel semi-circular ultra wide-band antenna for broadband applications that was inspired by a complementary split-ring resonator for bandwidth enhancement and a frequency selective surface reflector for gain enhancement, achieving a large bandwidth of 130.3 percent from 3.16 to 15 GHz and gain ranging from 4.9 dB to 10.9 dB. A simple low-profile defected ground structure-based monopole circular-shaped patch antenna for ultra-wideband applications was developed by Gopil et al. [27]. The antenna has an impedance bandwidth of 8.1GHz (2.5 – 10.6 GHz). For the two resonant frequencies, the gains are 8.4 dBi and 8.2 dBi, respectively. A rectangular microstrip patch antenna was designed by Kharusi et al. [28] for gain improvement using the air gap technique. The gain is increased from 6.907 dB to 9.179 dB based on the simulation results. E. K. I. Hamad and G. Nady [29] used metamaterial (MTM) double-side planar periodic structures to design a compact extended bandwidth UWB microstrip antenna. The antenna has a wide bandwidth of 3.2 to 23.9 GHz and a peak gain of 6.2 dB at 8.7 GHz.

III. ANTENNA DESIGN

The proposed rectangular microstrip patch antenna (RPMA) without and with slots are shown in Fig. 2, those are designed on FR4 dielectric substrate, having thickness of 0.8 mm with relative permittivity of 4.4 and the tangent loss of 0.02. The designed antenna is 30 mm × 20 mm in size. To excite the patch, the microstrip feed line is used with a characteristic impedance of 50 Ω. The RPMA without slots provides a narrow bandwidth of 3.68 GHz (3.24 GHz – 6.92 GHz) and a maximum gain of 5.06 dB, which are shown in Fig. 3(a) and (b). In order to increase the antenna bandwidth and gain, rectangular- right angle triangular slots are inserted into the patch and a single rectangular slot is added into the top edge of the partial ground plane. The various optimized parameters of the proposed antenna are mentioned in Table 1. The parameters have been obtained after several series of optimizations using HFSS.



(a) Side view

(b) RPMA without slots

(c) RPMA with slots

FIGURE 2. Design of the proposed rectangular patch microstrip antenna (RPMA).

TABLE 1. Design parameters value of the proposed antenna.

Parameters	Values (mm)	Parameters	Values (mm)
$W_S = W_g$	20	L_{g1}	3
L_S	30	L_{p1}	8
h	0.8	$L_{p5}=L_{p6}=W_{p2}=W_{p3}=W_{p4}$	0.5
W_p	18	$L_{p2}=L_{p3}=L_{p4}$	7
$L_p = L_g$	14	$W_{p5}=W_{p6}$	6.5
L_f	15	$p = q$	6
$W_f = W_{g1} = W_{p1}$	2	r	8.48

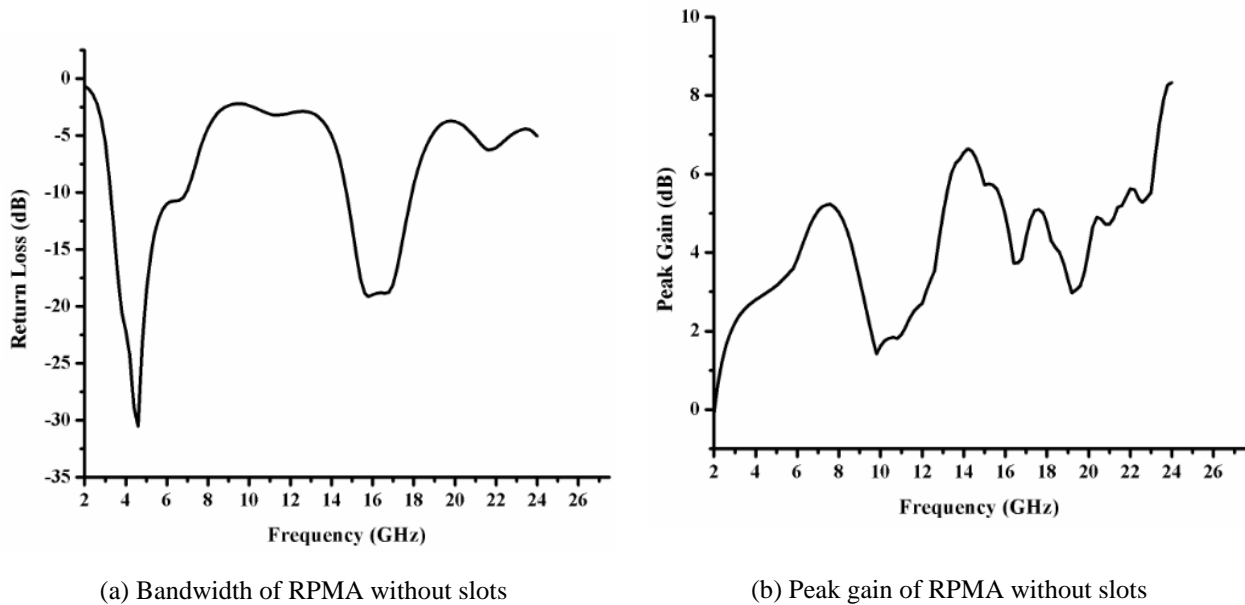


FIGURE 3. Bandwidth and peak gain of rectangular microstrip patch antenna (RPMA) design without slots.

IV. RESULTS AND DISCUSSIONS

The proposed antenna is simulated using Ansoft HFSS, and its numerical analysis is based on the finite element method. The bandwidth of an antenna is defined as the frequency range within which the performance of the antenna integrates to a specified standard with respect to certain characteristics. From the return loss graph, it can be calculated within the entire frequency range where the return loss remains below -10 dB.

The bandwidth of the rectangular patch microstrip antenna (RPMA) without and with slots is shown in Fig.4. We can observe from the figure that the RPMA without slots consists of two bands (3.24 – 6.92 GHz, and 14.69 – 17.91 GHz). The first band is of 3.68 GHz bandwidth (bandwidth percentage of 72.44%) and the graph clearly shows that the good performance of the antenna is at 4.55 GHz frequency where the return loss is -30.40 dB. The rectangular patch microstrip antenna (RPMA) with slots i.e. the slotted RPMA has an overall bandwidth of 19.7 GHz (3.15 GHz – 22.85 GHz) with nine resonance frequencies of 3.5 GHz, 6.3 GHz, 6.8 GHz, 7.7 GHz, 11.7 GHz, 15 GHz, 17.7GHz, 20 GHz, and 21.8 GHz and the graph also demonstrates that the good performance of the slotted RPMA is at 7.7 GHz with return loss of -28.35 dB. However, approximately 5.35 times wider bandwidth has been achieved compared to the RPMA without slots is shown in Fig. 4.

The different resonant frequencies of the proposed antenna can be used in various applications such as WiMAX technology (3.4 – 3.69) GHz, STM band applications (6 – 6.17 GHz), uplink (5.925 - 6.425 GHz) satellite communication, WLAN applications (5.15 – 5.825 GHz), radio astronomy applications (5.01 – 5.03 GHz), WiMAX (5.25 – 5.85 GHz) and C-band (4 – 8 GHz), downlink X-band satellite communication (7.25 – 7.75 GHz), and fixed-satellite service from space to earth (10.7 – 11.7 GHz), X-band (8 – 12 GHz) applications, amateur radio operations (10-10.5 GHz) and amateur satellite operations (10.45 – 10.5 GHz), and Ku band (12 – 18 GHz) applications.

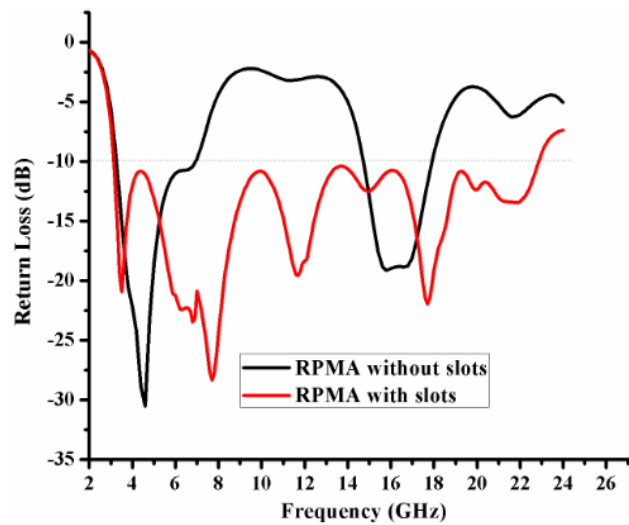


FIGURE 4. Comparison of return loss graphs of the rectangular patch microstrip antenna (RPMA) without and with slots.

Gain is a measure of the capability of an antenna to concentrate the transmitted energy in a specific direction. The peak gain plot of the rectangular microstrip patch antenna (RPMA) without slots and rectangular microstrip patch antenna (RPMA) with slots is shown in Fig.5. The gain of the slotted rectangular patch microstrip antenna (SRPMA) increases as the frequency increases. Because of the shorter wavelength at high frequencies, the effective area of the antenna increases. It is clearly noticeable from the figure that the peak gain of the SRPMA is 8.06 dB means that 5.5 times the amount of effective power will be sent in the direction of a target than from an isotropic radiator, and so has the equivalent effect of eight times the power of the transmitter in that particular direction, while the peak gain of the RMPA is 5.06 dB means that 3.50 times more effective power is sent in the direction of a destination than from an isotropic radiator, and thus has the equal impact of 3.50 times the energy of the transmitter in that specific direction. From the above gain discussion, it is clear that the gain of the slotted RPMA is 3 dB greater than that of the rectangular patch microstrip antenna (RPMA).

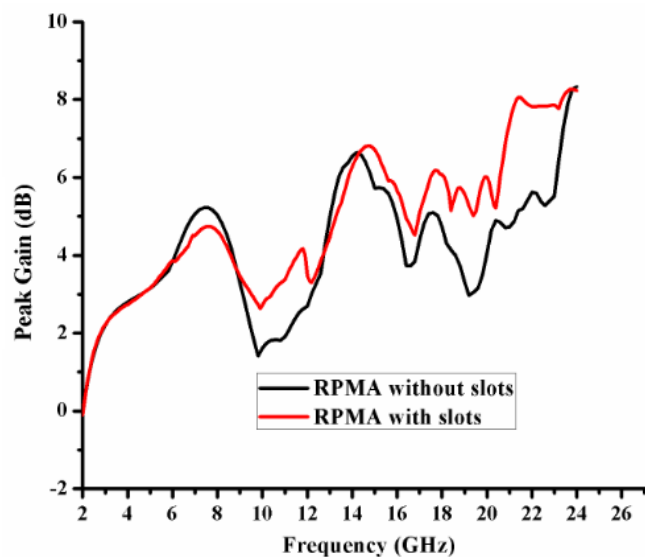


FIGURE 5. Comparison of peak gain graphs of the rectangular patch microstrip antenna (RPMA) without and with slots.

Figure 6(a) and (b) depict a simulated 2D view of the far-field radiation pattern of a rectangular patch microstrip antenna (RPMA) without and with slots at 6.85 GHz, respectively. The radiation patterns of the antenna in the E-plane



and H-plane are similar to those of a dipole antenna at the resonance frequency of 6.85 GHz.

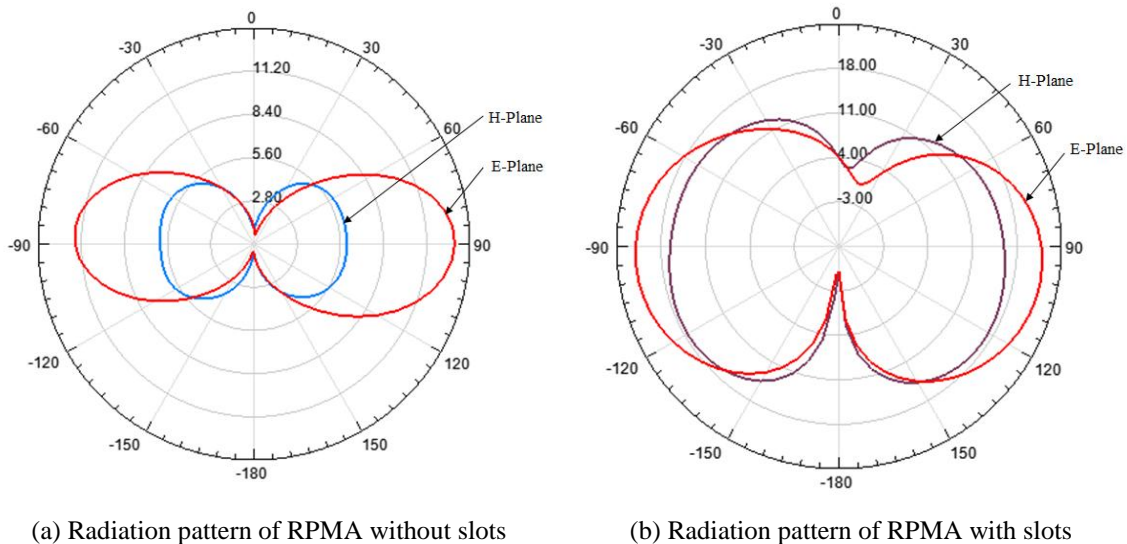


Figure 6. 2D view of the far field radiation pattern of rectangular patch microstrip antenna (RPMA) design.

The effects of a rectangular patch microstrip antenna (RPMA) without slots are investigated. The surface current distribution density of the RPMA without slots is simulated at 6.85 GHz and is shown in Fig. 7(a). Similarly, the surface current distribution density of the RPMA with slots is simulated at 6.85 GHz and is shown in Fig. 7(b). The current flow of the RPMA with slots at 6.85 GHz is found to be greater than the current flow of the RPMA without slots based on the current surface distribution. This enhances the antenna's capacity and gain.

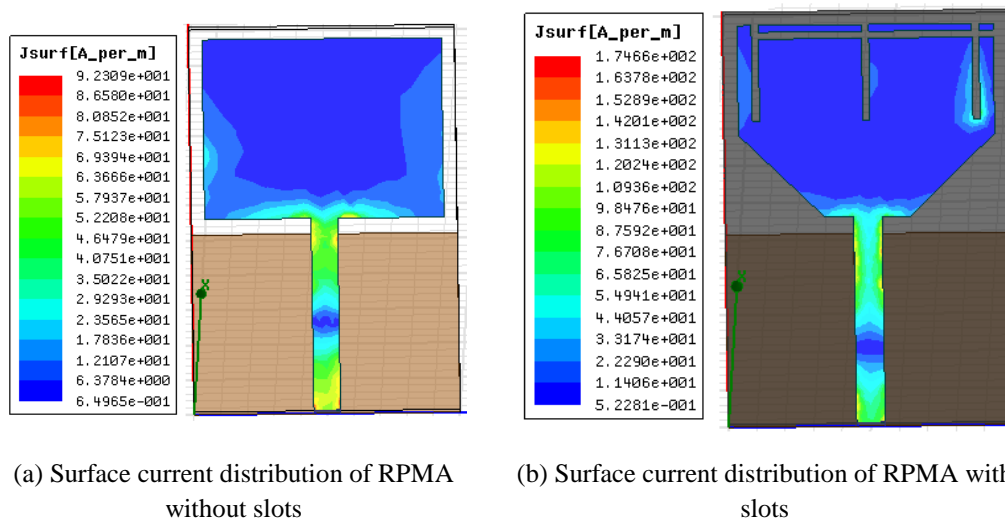


FIGURE 7. Distributions of surface current of rectangular patch microstrip antenna (RPMA) at 6.85 GHz.

A comparison of the bandwidth, bandwidth percentage, and gain of the proposed rectangular patch microstrip antenna (RPMA) without slots and with slots is shown in Table 2. From the table it is seen that the bandwidth of the RPMA with and without slots is 19.7 GHz and 3.68 GHz respectively. Bandwidth increases from 3.68GHz to 19.7 GHz. There is a 79.1% improvement in bandwidth. The gain of the RPMA with and without slots is 5.06 dB and 8.06 dB, respectively i.e. there is an increase of 3 dB in gain for the slotted patch antenna. It is clear from Table 2 that, the



bandwidth and gain of the proposed RPMA with slots has been improved significantly as compared to the RPMA without slots.

TABLE 2. Comparison of bandwidth, bandwidth percentage and gain of the proposed rectangular microstrip patch antenna (RPMA) without and with slots.

Parameters	RPMA without slots	RPMA with slots	Improvement factor
Bandwidth	3.68 GHz (3.24 GHz – 6.92 GHz)	19.7 GHz (3.15 GHz – 22.85 GHz)	16.02 GHz
Bandwidth percentage	72.44%	151.54%	79.1 %
Gain	5.06 dB	8.06 dB	3 dB

VI.CONCLUSION

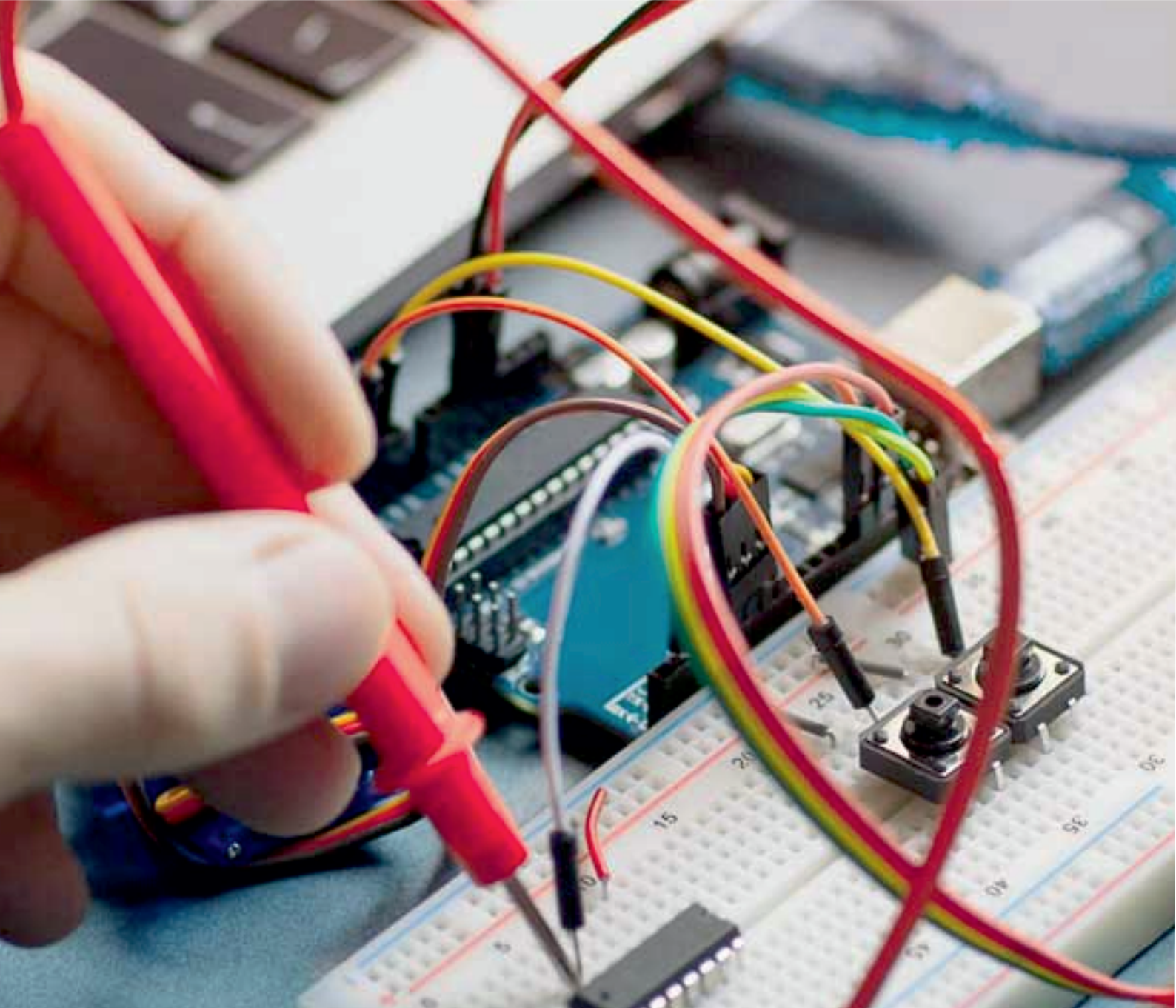
The main disadvantages of the microstrip patch antenna are its restricted bandwidth and low gain, which limit its application. The proposed antenna overcomes these implicit constraints by including rectangular-right angle triangle-shaped slots on the patch and a single rectangular shaped slot on the partial ground plane. This designed antenna improves both bandwidth and gain. The analysis shows that the bandwidth of the rectangular patch microstrip antenna without slots (conventional antenna) has increased from 72.44% to 151.54%, which means 79.1% improvement in bandwidth by using slots into the patch-partial ground plane. The gain has also improved from 5.06 to 8.06 dB.

REFERENCES

- [1] I. Singh and Tripathi, "Microstrip patch antenna and its application: A survey," International Journal of Computer Technology and Applications, vol. 2, no. 5, pp. 1595- 1599, 2011.
- [2] H. Srivastava, A. Singh, A. Rajeev, and Tiwari, "Comparison of different microstrip patch antennas with proposed RMPA for wireless applications," International conference on power electronics, control and automation (ICPECA), New Delhi, India, pp.1- 4, 2019.
- [3] H. Kaur and Kaur, "Design of microstrip patch circular antenna using microstrip line feed technique," International Journal for Research in Applied Science and Engineering Technology (IJRASET), 6(X), pp. 1- 8, 2018.
- [4] R. Garg, P. Bartia, I. Bahl, and Ittipiboon, Microstrip antenna design handbook. Norwood, MA: Artech House Inc. A., pp. 253 – 316, 2001.
- [5] L. C. Paul, M. S. Hosain, S. Sarker, M .H Prio, M. Morshed, and Sarkar, "The effect of changing substrate material and thickness on the performance of inset feed microstrip patch antenna," American Journal of Networks and Communications, vol. 4, no. 3, pp. 54 – 58, 2015.
- [6] D. Guha, S. Chattopadhyaya, and Siddiqu, "Estimation of gain enhancement replacing PTFE by air substrate in a microstrip patch antenna [antenna designer's notebook]," IEEE Antennas and Propagation Magazine, vol. 52, no. 3, pp. 92- 95, 2010.
- [7] A. F. Darweesh and G. O. Yetkin, "Enhancement of the gain and the bandwidth of a UWB microstrip patch antenna using metamaterials," International Journal of Engineering & Technology, vol. 7, pp. 380–385, 2018.
- [8] J. Vijayalakshmi and G. Murugesan, "A Miniaturized High-Gain (MHG) Ultra-Wideband Unidirectional Monopole Antenna for UWB Applications," Journal of Circuits, Systems and Computers, vol. 28, no. 4, pp. 1-16, 2019.
- [9] S. Patel and C. Argyropoulos, "Enhanced bandwidth and gain of compact microstrip antennas loaded with multiple corrugated split ring resonators," Journal of Electromagnetic Waves and Applications, vol. 30, no. 7, pp. 945 – 961, 2016.
- [10] M. Samsuzzaman, M. T. Islam, and J. S. Mandeep, "Design of a compact new shaped microstrip patch antenna for satellite application," Adv Nat Appl Sci., vol. 6, no. 6, pp. 898- 903, 2012
- [11] S. M. Abbas, I. Saleem, B. Ahmed, and H. Khurshid, "UWB antenna with parasitic and asymmetric feed," Information Science Letters, vol. 2, no. 1, pp. 27- 33, 2013.
- [12] S. Baudha and M. V. Yadav, "A compact ultra-wideband planar antenna with corrugated ladder ground plane for multiple applications," Microwave and Optical Technology Letters, vol. 61, no. 4, pp. 1- 8, 2019.



- [13] S. Baudha and M. V. Yadav, "A novel design of a planar with modified patch and defective ground plane for ultra-wideband applications," *Microwave and Optical Technology Letters*, vol. 61, no. 5, pp. 1- 8, 2019.
- [14] K. G. Tan, S. Ahmed, A. Hamdi, C. X. Ming, K. Abdulwasie, et al., "FR-4 Substrate Based Modified Ultrawideband Antenna with Gain Enhancement for Wireless Applications," *Journal of Engineering Science and Technology Review*, vol. 12, no. 4, pp. 108 – 112, 2019.
- [15] S. Elajoumi, A. Tajmouati, J. Zbitou, A. Errkik, A. M. Sanchez, and M. Latrach, "Bandwidth enhancement of compact microstrip rectangular antennas for UWB applications," *Telkomnika*, vol. 17, pp. 1559- 1568, 2019.
- [16] R. D. Mishra and P. K. Singha "Gain Enhancement of Rectangular Microstrip Patch Antenna Designed for Exposure System Using Microstrip Array," *International Journal of Signal Processing, Image Processing and Pattern Recognition*, vol. 9, no. 5, pp. 417- 430, 2016.
- [17] H. Xiong, J. S. Hong, and Y. H. Peng, "Impedance Bandwidth and Gain Improvement for Microstrip Antenna using Metamaterials," *Radioengineering*, vol. 21, no. 4, pp. 993- 998, 2012.
- [18] A. A. Roy, J. M. Môm, and Igwue, "Enhancing the Bandwidth of a Microstrip Patch Antenna Using Slots Shaped Patch," *American Journal of Engineering Research (AJER)*, vol. 2, pp. 23- 30, 2013.
- [19] Y. Sung, "Bandwidth enhancement of a microstrip line-fed printed wide-slot antenna with a parasitic center patch," *IEEE Trans. Antennas Propag.*, vol. 60, no. 4, pp. 1712-1716, 2012.
- [20] A. Ghosh and S. Das, "Gain Enhancement of Slot Antenna using Laminated Conductor Layers," *International Conference on Devices, Circuits and Communications (ICDCCom)*, Ranchi, India, pp. 1- 4, 2014.
- [21] X. Zhao, Y. Huang, J. Li, Q. Zhang, and G. Wen, "Wideband High Gain Circularly Polarized UHF RFID Reader Microstrip Antenna and Array," *AEU- International Journal of Electronics and Communications*, vol. 77, pp. 76- 81, 2017.
- [22] Y. F. Lin, M. J. Chang, H. M. Chen, and B. Y. Lai, "Gain Enhancement of Ground Radiation Antenna for RFID Tag Mounted on Metallic Plane," *IEEE Transactions on Antennas and Propagation*, vol. 64, pp. 1193- 1200, 2016.
- [23] M. A. Amiri, C. A. Balanis, and C. Birtcher, "Gain and Bandwidth Enhancement of a Spiral Antenna using a Circularly Symmetric HIS," *IEEE Antennas and Wireless Propag. Lett.*, vol. 16, pp. 1080-1083, 2017.
- [24] D. Rusdiyanto, C. Apriono, D. W. Astuti, and Muslim, "Bandwidth and Gain Enhancement of Microstrip Antenna using Defected Ground Structure and Horizontal Patch Gap," *Sinergi*, vol. 25, pp. 153-158, 2021.
- [25] G. V. Raviteja, B. T. V. Madhan, M. K. Sree, N. Avinash, and P. R. S. Naga Surya, "Gain and Bandwidth Considerations for Microstrip Patch Antenna Employing U and Quad L shaped Slots with DGS and Parasitic Elements for WiMax / WiFi Applications," *EJERS, European Journal of Engineering Research and Science*, vol. 5, pp. 327- 330, 2020.
- [26] A. Swetha and K. R. Naidu, "Gain Enhancement of an UWB Antenna Based on a FSS Reflector for Broadband Applications," *Progress In Electromagnetics Research C*, vol. 99, pp. 193- 208, 2020.
- [27] D. Gopil, A. R. Vadaboyina, and J. R. K. K Dabbakuti, "DGS based monopole circular-shaped patch antenna for UWB applications," *SN Appl. Sci.* vo. 3, no. 2, 198, 2021, doi: 10.1007/s42452-020-04123-w.
- [28] K. W. S. A. Kharusi, N. Ramli, S. Khan, M. T. Ali, and M. H. A. Halim, "Gain Enhancement of Rectangular Microstrip Patch Antenna using Air Gap at 2.4 GHz," *International Journal of Nanoelectronics and Materials*, vol. 13, pp. 211- 224, 2020.
- [29] E. K. I. Hamad and G. Nady, "Bandwidth Extension of Ultra-wideband Microstrip Antenna using Metamaterial Double-side Planar Periodic Geometry," *Radioengineering*, vol. 28, pp. 25- 32, 2019.



INNO SPACE
SJIF Scientific Journal Impact Factor
Impact Factor: 7.282



ISSN INTERNATIONAL
STANDARD
SERIAL
NUMBER
INDIA



International Journal of Advanced Research

in Electrical, Electronics and Instrumentation Engineering

 **9940 572 462**  **6381 907 438**  **ijareeie@gmail.com**



www.ijareeie.com

Scan to save the contact details



Review on Flexible Power Point Tracking Based Frequency Regulation Strategy for PV

Shivani Mungase, Pawan Tapre

Dept. of Electrical Engineering (Power System), SND College of Engineering Yeola, Nashik, India

Dept. of Electrical Engineering (Power System), SND College of Engineering Yeola, Nashik, India

ABSTRACT: In this study maximum power point tracking (MPPT) is applied to the photovoltaic (PV) system to harvest the maximum power output. The output power of the PV effect changes according to external solar irradiation and ambient temperature conditions. In the existing MPPT strategies, most of them only take variations in radiation level into account, rarely considering the impact of temperature changes. Unlike existing strategies, irradiance information and complex model estimation are not required, except for the maximum power curve. The suboptimal power point at any irradiance and reserve ratio can be automatically converged with the proposed tracking method. Furthermore, an adaptive step-size tracking method is proposed to improve the output power fluctuation around the suboptimal power point.

KEYWORDS: maximum power point tracking (MPPT); photovoltaic (PV) system; fuzzy logic control (FLC)

I. INTRODUCTION

With the development of photovoltaic (PV) technologies, an increasing number of PV power generation systems have been presented for large-scale applications. The PV module is one of the key components of PV power generation systems; its performance and efficiency directly affect the high-efficiency operation of the entire system. However, the power energy generated from PV modules relies highly on environmental factors such as solar insulation and the ambient temperature. Therefore, in order to harvest the maximum power output and improve the efficiency of the entire PV system, many advanced MPPT control methods have been implemented in PV systems.

Many MPPT control algorithms have been proposed and developed in recent years, such as the classic methods, including open-circuit voltage (OCV)/short-circuit current (SCC), incremental conductance (INC), perturbation-and-observation (P&O) and other hybrid strategies. Due to the non-linear problems of PV cells, some soft computing techniques have been applied to the MPPT of PV systems, such as the artificial neural networks method (ANN) and fuzzy logic control (FLC). Most of the MPPT approaches only take the variability in radiation level into account, while rarely considering the effects of temperature. Some new MPPT methods based on temperature measurements were discussed in Reference. Many control algorithms use temperature as a feedback parameter to realize MPPT. For example, studies in References proposed an MPPT-temperature algorithm where the PV module temperature was used to determine the maximum power point voltage to track the maximum power point (MPP). In Reference, a sun tracking system that included the temperature effect was presented, and an optimum system design was achieved. Compared to other approaches under the same control algorithm, the MPPTs based on temperature measurement directly consider the temperature variations leading to MPP changes, which can obtain a faster tracking speed, especially in engineering applications where temperature changes are relatively large. Furthermore, to improve the tracking accuracy, some artificial intelligence techniques have been employed for the MPPT implementation. Fuzzy logic control (FLC) is a relatively popular and mature artificial intelligence algorithm and has been applied to track the MPP in PV systems.

II. LITERATURE SURVEY

In [1], a frequency regulation control strategy based on FPPT was proposed. The simulation results of the different scenarios verify its effectiveness and correctness. The proposed FPPT method can automatically converge to the suboptimal power point at any irradiance conditions while irradiance information is not required. The FPPT method does not require complex model estimation and is easy to implement. The algorithm only must know the maximum power curve; the suboptimal power curve can be obtained by the transformation from the maximum power curve. The simulation results show that the proposed strategy can track a given power reserve ratio quickly and robustly. The variation step tracking controller is designed to smooth the output power, with only a slight reduction in tracking speed. Based on the FPPT method, the frequency regulation strategy for a PV system has been proposed. The strategy changes the reserve ratio to participate in grid frequency variation, increasing or decreasing the output power. The simulation



results show that the proposed frequency regulation strategy can significantly improve the frequency response of a system with a PV plant.

In [2], an overview of several FPPT algorithms in the literature has been provided. A short description of the algorithms is provided, while their features are comprehensively compared. Experimental results are also illustrated to analyze the dynamic performance of these algorithms. Based on the results, the FPPT algorithms that directly calculate the PV voltage reference, corresponding to the PV power reference, demonstrate a better overall performance in various aspects. These algorithms do not necessitate multi-mode transitions between different operation modes, while they are flexible to move the operation point of the PV string to the right- or left-side of the MPP. Fast dynamic response and low power oscillations in steady state can also be achieved by adaptively calculating the voltage-step in these algorithms. Furthermore, they do not compel any change in the voltage control block of the PVPPs.

In [3], an algorithm is proposed for determining the reference voltage of the PV string which results in a reduction of the output power to a certain amount. The proposed algorithm calculates the reference voltage for the dc/dc converter controller, based on the characteristics of the power-voltage curve of the PV string and therefore, no modification is required in the the controller of the dc/dc converter. Simulation results on a 50-kW PV string verified the effectiveness of the proposed algorithm in reducing the power from PV strings under different irradiation and reference power values

. In [4], a costeffective solution to realize delta power control for grid-connected PV systems is presented, where the multi-string PV inverter configuration is adopted. This control strategy is a combination of Maximum Power Point Tracking (MPPT) and Constant Power Generation (CPG) modes. In this control scheme, one PV string operating in the MPPT mode estimates the available power, while the other PV strings regulate the total PV power by the CPG control strategy in such a way that the delta power constraint for the entire PV system is achieved. Simulations and experiments have been performed on a 3-kW single-phase grid-connected PV system. The results have confirmed the effectiveness of the proposed delta power control strategy, where the power reserve according to the delta power constraint is achieved under several operating conditions.

In [5], a multi-mode FPPT algorithm for GCPVPPs has been introduced. The operation mode of the proposed algorithm is selected based on comparing the PV power with the desired power reference. If the PV power is larger than the power reference, an additional value Δv is added to the voltage of the MPP to facilitate operation on the right-side of the MPP. Similarly, Δv is subtracted from the voltage of the MPP to facilitate operation on the left-side of the MPP. Since the additional voltage value is calculated based on the error between the PV power and the power reference, fast dynamics are obtained. If the PV power is smaller than its reference value, a conventional MPPT algorithm is applied to increase the PV power by moving its operation point towards the MPP.

In [6], a control algorithm to limit the inverter peak current and achieve zero active power oscillation for the GCPVPP during unbalanced voltage sags has been introduced and investigated. The main contribution of this study is to derive an analytical expression for P^* and Q^* that can be implemented in combination with various current reference calculation algorithms. It also ensures that the inverter peak current remains within its nominal value. Since the amplitudes of the phase current references depend on the voltage positive- and negative-sequences, a rescaling factor (K_{rs}) was applied in order to ensure the operation of the inverter within its nominal range.

In [7], imprinted AgNW transparent electrode that possesses high transmission and low resistance has been developed. The imprinted AgNW thin film is utilized to replace the ITO layer to fabricate the flexible PVKs. The flexible PVKs were further combined with maximum power point tracking (MPPT) algorithms to improve the power consumption. The PCE of the flexible ITO-free PVKs can reach 8.0%.

In [8], a method to control the dc-dc converter of GCPVPPs has been introduced. The proposed algorithm uses dynamic voltage reference design as the voltage control technique and calculates the average inductor current reference, and uses the model predictive control to regulate the current and to calculate the duty cycle of the dcdc converter. The applicability and effectiveness of the proposed technique have been demonstrated by the simulation and experimental results. Fast dynamic response is achieved under a change in the PV reference power and under unbalanced grid voltage condition. The proposed control scheme is sought to be a more flexible method that produces faster transient performance with satisfactory steady state response.

In [9], an algorithm for the control of cascaded H-bridge (CHB)-based PV systems to achieve frequency response for them is proposed. The required power reference, based on the grid operation condition, is distributed among the sub-modules (SMs) of the CHB converter considering the available power from each SM and operational constraints of the system. The details of the proposed control algorithm are provided, while its effectiveness is evaluated on a 1.5-MW PV simulation setup, connected directly to a 6.6-kV grid.

In [10], the design and development of particle swarm optimization (PSO) based maximum power point tracking (MPPT) algorithm for photovoltaic energy conversion system is described. The proposed MPPT is simple, flexible, accurate and efficient in maximum photovoltaic power tracking. In this work, MATLAB/Simulink simulation package



is used to simulate the performance of the proposed MPPT algorithm. The performance of the proposed PSO algorithm is evaluated by comparing it with the conventional P&O method in terms of tracking speed and accuracy. The simulation results demonstrate that the tracking capability of the PSO algorithm is more efficient, comparing to the traditional one, particularly under parameters variation conditions.

III. PROPOSED SYSTEM

The proposed FPPT control strategy introduces a maximum power tracking curve. Power electronic converters are commonly applied in a PV system to achieve different MPPT control methods, where the converters act as the interface between the PV source and different loads. In order to efficiently track the MPP, the converter needs to adjust the duty cycle under varying operating atmospheric conditions. The MPPT controller (Fuzzy logic controller) acquires the real-time operating parameters depending on the control algorithm, then outputs the corresponding control signal to control the DC/DC converter. The most common solar PV MPPT system consists of a PV module, DC/DC boost converter, MPPT controller and a load, as shown in Figure 1. The PV cells generate power energy and its output is connected to the DC/DC converter. The converter is controlled by the MPPT controller where different control algorithms can be carried out.

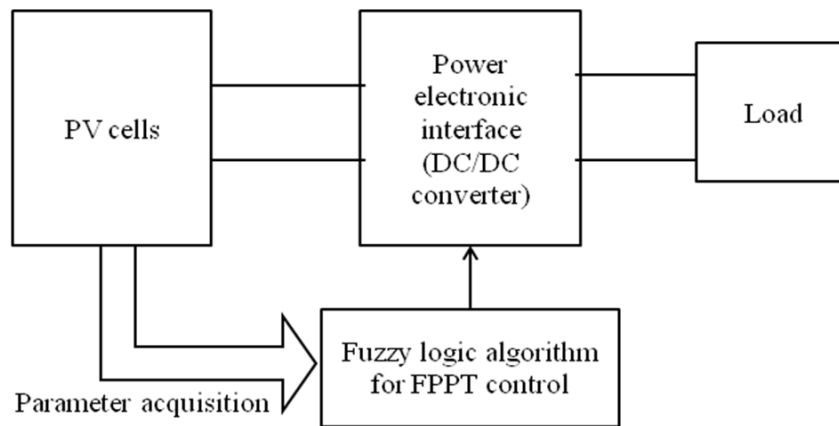


Fig 1 block diagram of proposed system

Due to the nonlinear characteristics of the PV system, intelligent MPPT control algorithms in PV systems are very promising and some have been successfully employed for maximum power extraction. Fuzzy logic control (FLC) is one of the most prevalent intelligent control techniques, which has advantages like a fast response time, less fluctuation and high control accuracy. Therefore, it is effective in controlling nonlinear systems.

IV. CONCLUSION

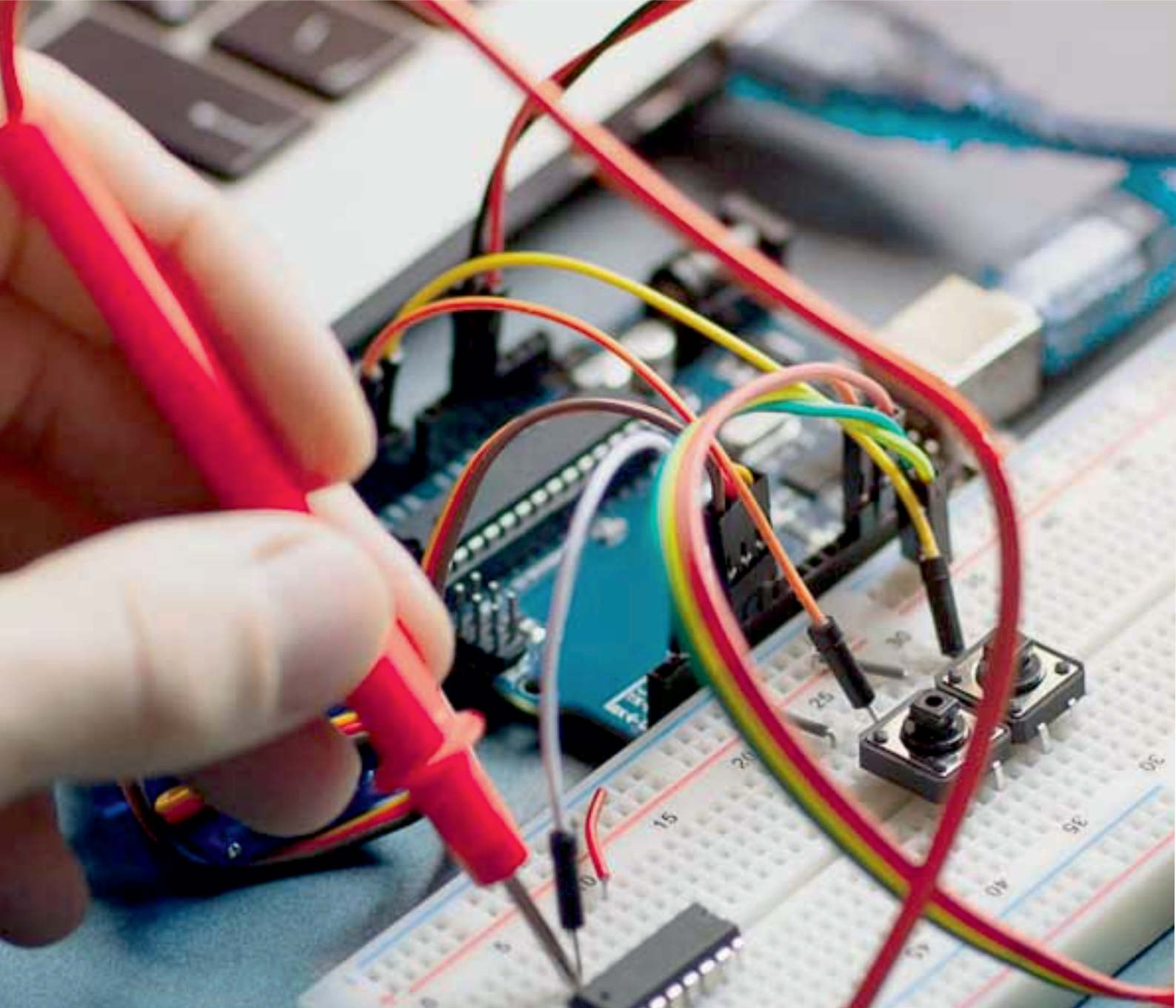
In this study, a FLC based on FPPT was proposed. The simulation results of the different scenarios verify its effectiveness and correctness. The FPPT method does not require complex model estimation and is easy to implement. The algorithm only must know the maximum power curve; the suboptimal power curve can be obtained by the transformation from the maximum power curve. The simulation results show that the proposed strategy can track a given power reserve ratio quickly and robustly.

REFERENCES

- [1] Zhong, C., Zhou, Y., Zhang, X.-P., & Yan, G. (2020). Flexible power-point-tracking-based frequency regulation strategy for PV system. *IET Renewable Power Generation*, 14(10), 1797–1807. doi:10.1049/iet-rpg.2020.0013
- [2] Tafti, H. D., Konstantinou, G., Townsend, C. D., Farivar, G. G., Sangwongwanich, A., Yang, Y., ... Blaabjerg, F. (2019). A Comparative Study of Flexible Power Point Tracking Algorithms in Photovoltaic Systems. 2019 IEEE 4th International Future Energy Electronics Conference (IFEEC). doi:10.1109/ifeec47410.2019.9015107
- [3] Tafti, H. D., Maswood, A. I., Pou, J., Konstantinou, G., & Agelidis, V. G. (2016). An algorithm for reduction of extracted power from photovoltaic strings in grid-tied photovoltaic power plants during voltage sags. *IECON 2016 - 42nd Annual Conference of the IEEE Industrial Electronics Society*. doi:10.1109/iecon.2016.7793187
- [4] Sangwongwanich, A., Yang, Y., Blaabjerg, F., & Sera, D. (2017). Delta Power Control Strategy for Multistring Grid-Connected PV Inverters. *IEEE Transactions on Industry Applications*, 53(4), 3862–3870. doi:10.1109/tia.2017.2681044



- [5] Dehghani Tafti, H., Townsend, C. D., Konstantinou, G., & Pou, J. (2018). A Multi-Mode Flexible Power Point Tracking Algorithm for Photovoltaic Power Plants. IEEE Transactions on Power Electronics, 1–1. doi:10.1109/tpel.2018.2883320
- [6] Dehghani Tafti, H., Maswood, A. I., Konstantinou, G., Pou, J., & Acuna, P. (2018). Active/reactive power control of photovoltaic grid-tied inverters with peak current limitation and zero active power oscillation during unbalanced voltage sags . IET Power Electronics, 11(6), 1066–1073. doi:10.1049/iet-pel.2017.0210
- [7] Ming-Yi Lin Shih-Lun Chen, “Fabrication of Imprinted Flexible Solar PV Maximum Power Point Tracking System for Smart Cities Sustainable Development”, 2018 1st International Cognitive Cities Conference (IC3) 978-1-5386-5059-2/18/\$31.00 ©2018 IEEE DOI 10.1109/IC3.2018.00-29
- [8] Narang, A., Tafti, H. D., Townsend, C. D., Farivar, G., Pou, J., Konstantinou, G., & Vazquez, S. (2019). An Algorithm for Fast Flexible Power Point Tracking in Photovoltaic Power Plants. IECON 2019 - 45th Annual Conference of the IEEE Industrial Electronics Society. doi:10.1109/iecon.2019.8927083
- [9] Hossein Dehghani Tafti(1, *), Georgios Konstantinou(1), John E. Fletcher(1) , Glen G. Farivar(2), Salvador Ceballos(2, 3), Josep Pou(2, 4) and Christopher D. Townsend, “Flexible Power Point Tracking in Cascaded H-Bridge Converter-Based Photovoltaic Systems”, 978-1-7281-5414-5/20/\$31.00 ©2020 IEEE
- [10] Soufi, Y., Bechouat, M., & Kahla, S. (2018). Particle Swarm Optimization Based Maximum Power Point Tracking Algorithm for Photovoltaic Energy Conversion System. 2018 15th International Multi-Conference on Systems, Signals & Devices (SSD). doi:10.1109/ssd.2018.8570633



INNO SPACE
SJIF Scientific Journal Impact Factor
Impact Factor: 7.282



ISSN INTERNATIONAL
STANDARD
SERIAL
NUMBER
INDIA



International Journal of Advanced Research

in Electrical, Electronics and Instrumentation Engineering

 **9940 572 462**  **6381 907 438**  **ijareeie@gmail.com**



www.ijareeie.com

Scan to save the contact details